

# Impact fracture of crystalline, Ar<sup>+</sup>-amorphized, and amorphous silicon dioxide

© I.P. Shcherbakov, A.E. Chmel

Ioffe Institute,  
194021 St. Petersburg, Russia  
e-mail: chmel@mail.ioffe.ru

Received September 10, 2021

Revised November 12, 2021

Accepted November 18, 2021

The mechanical fracture of silicon dioxide initiates the mechanoluminescence (ML) lighting due to multiple breakage of interatomic bonds with producing non-bridged oxygen groups of  $[\equiv\text{Si}-\text{O}^-]$ . The detected ML signals consisted of series of pulses, the energy of which is proportional to the number of photons irradiated from the broken bonds. The comparative analysis of the energy distributions in ML series induced by the impact damage of the surface of crystalline and vitreous  $\text{SiO}_2$  before and after the Ar<sup>+</sup>-ion implantation was conducted. The interplay between random and correlated accumulation of broken bonds under the impact loading was found and discussed.

**Keywords:** silicon dioxide, Ar<sup>+</sup>-implantation, impact damage, mechanoluminescence.

DOI: 10.21883/TP.2022.02.52952.254-21

## Introduction

The structure of amorphous (vitreous) silicon dioxide,  $v\text{-SiO}_2$ , is an endless mesh of disorderly linked six-membered rings made up of  $\text{SiO}_4$  tetrahedra. Optical and mechanical properties are fully isotropic.

Crystalline quartz ( $\alpha\text{-SiO}_2$ ) has a regular anisotropic structure in the form of tetrahedra located in helical fashion in relation to the crystal main axis; the crystal shape is a hexagonal prism. The long-range order in  $\alpha\text{-SiO}_2$  can be destroyed by neutron bombardment or implantation of ions which create multiple stable defects — broken interatomic bonds. The corresponding rearrangement of the crystalline structure was called „amorphization“  $\alpha\text{-SiO}_2$  [1–3]. However, though bombardment with particles destroys the long-range order in the crystal, amorphized quartz ( $\text{SiO}_2^{\text{amorphiz}}$ ) in terms of thermodynamics is not an amorphous (in other words, vitreous) substance [4]. During annealing, fused quartz retains the disordered structure, while amorphized quartz turns into a conventional crystal [5].

Crystalline quartz within quartz sand is the main component of materials for load-bearing structures and bio-protection facilities at nuclear power plants and other nuclear power units [6]. Therefore, the study of the amorphized state of  $\alpha\text{-SiO}_2$  crystals is of practical interest from the viewpoint of specificity of their mechanical properties.

In the present paper, specimens of both phase states were implanted with inert Ar<sup>+</sup> ions which, like neutrons, do not interact chemically with silicon dioxide, though the influence of neutral particles on the material is not purely mechanical. During ion bombardment of a dielectric specimen, implanted atoms generate an electric field under the surface which polarizes the near-surface layer [7].

Upon mechanical breakdown of silicon dioxide in the above-mentioned phase states, some interatomic bonds break up and defects with unbound oxygen form  $[\equiv\text{SiO}_2]$ , accompanied with light emission (mechanoluminescence, ML). Thus, ML pulses are indicators of elementary defects in  $\text{SiO}_2$ . The present paper describes the experiments in mechanical damage of the surface of crystalline, amorphized and vitreous (molten) silicon dioxide, where the fracture process was characterized by release of ML luminescence.

## 1. Specimens

Amorphous (vitreous)  $\text{SiO}_2$  was obtained by deposition in the flame of an oxygen-hydrogen burner. Crystalline quartz was synthesized by the hydrothermal method. Specimens of both phase states were prepared in the form of plates with polished surfaces, implanted with inert Ar<sup>+</sup> ions with the energy of 40 keV in the ILU 4 linear accelerator, at room temperature and with the current density of  $5\ \mu\text{A}/\text{cm}^2$ . Implantation dose ( $D$ ) was  $1 \cdot 10^{16}\ \text{Ar}^+/\text{cm}^2$ . The depth of the amorphized layer under these implantation conditions was 3–6 Å [8].

## 2. Equipment

The specimens were placed on a solid metal support coated with a layer of consistent grease. Damage was caused by the impact of a 100 g load, dropped from the height of 100 cm onto a sharpened stainless steel striker mounted on the specimen surface. This loading pattern provided a localized ( $\cong \text{Ø}1\ \text{mm}$ ) surface defect with a well-visible morphology of fracture of each material under testing.

ML illumination was collected by a quartz lens and directed to the FEU136 photomultiplier, signals from which

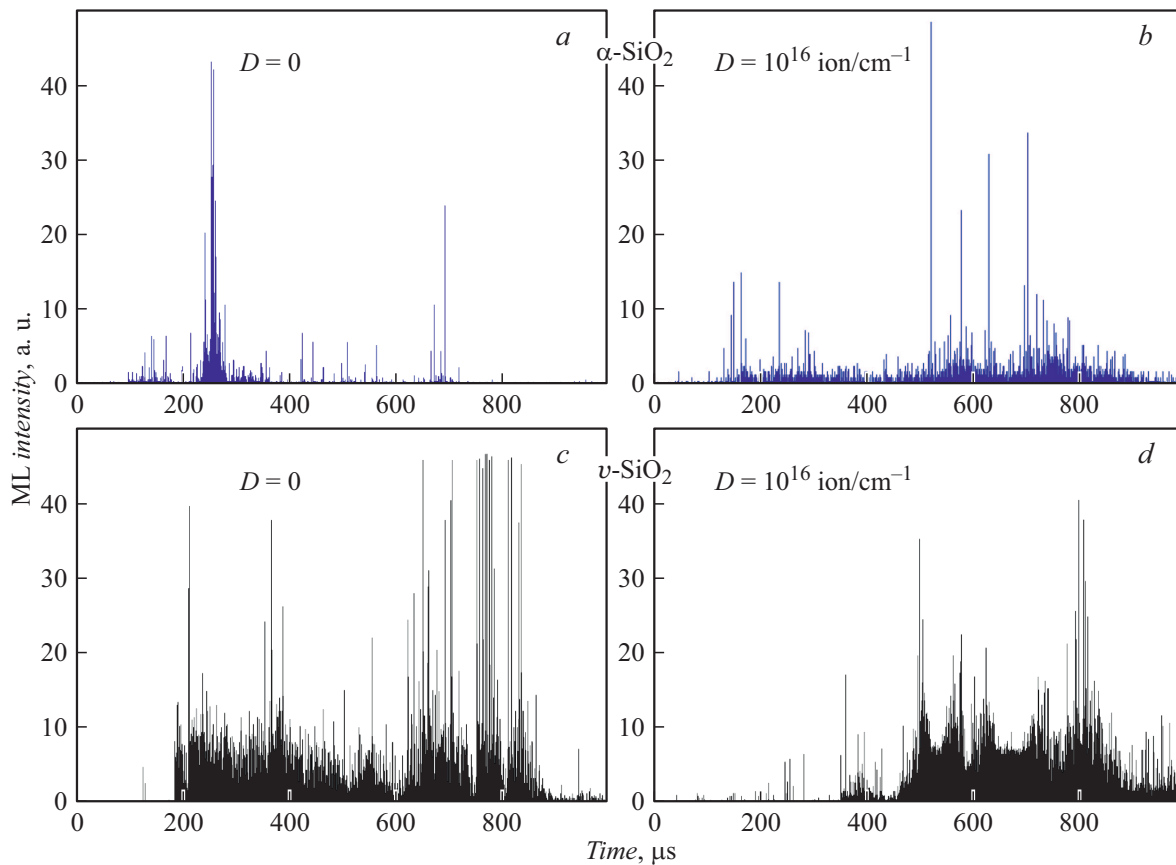


**Figure 1.** Time series of ML pulses formed upon impact loading of samples of  $\alpha$ -SiO<sub>2</sub> (a), SiO<sub>2</sub><sup>amorphiz</sup> (b),  $v$ -SiO<sub>2</sub> before (c) and after (d) ion implantation.

were sent to the input of the ASK-3106 analog-to-digital converter and saved in the computer. The duration of ML signal collection was 1 ms. The time resolution of pulses was 20 ns.

### 3. Mechanical impact

Fig. 1 shows the time sweeps of ML excited by a pinpoint impact in the specimens of  $v$ -SiO<sub>2</sub> and  $\alpha$ -SiO<sub>2</sub> before and after the implantation. A comparison of the sweeps shows a delay of the beginning of intensive luminescence in the implanted specimens as compared to the non-bombarded specimens. The effect is more pronounced in the vitreous material and appears to be due to the plastic flow at the initial loading stage, when bond breaks are insignificant. It has been already showed [9] that the morphology of damage under impact loading of  $v$ -SiO<sub>2</sub>, modified by ion implantation, has the signs of fracture of a plasticized material. In our case, Fig. 2, a, b shows that the craters of the non-bombarded crystalline and amorphous specimens have pronounced radial cracks typical for brittle fracture, while the  $\alpha$ -quartz, amorphized by implantation, shows a plastic flow of the crater edges (Fig. 2, c).

A difference in the pattern of damage to the amorphous and amorphized materials has also manifested itself in

distributions of intensity of luminescent glow from the loaded specimens. Energy ( $E$ ) in ML pulses is proportional to the number of photons emitted upon breaks of interatomic bonds. Fig. 3 shows the distributions of  $E$  in ML pulses for all the tested specimens in the form of plots of  $N(E > \varepsilon)$  vs.  $\varepsilon$ , where  $N$  is the number of pulses whose energy  $E$  is higher than certain threshold quantity  $\varepsilon$ , which successively takes on the values of energy in pulses (horizontal coordinate); the number of pulses whose energy  $E$  exceeds the current value of  $\varepsilon$  is plotted on the vertical axis.

The same data were plotted in two coordinates — semilogarithmic (Fig. 3, a, c) and double logarithmic (Fig. 3, b, d). The graph of energy distribution during testing of a non-bombarded specimen of  $\alpha$ -SiO<sub>2</sub> (Fig. 3, a), constructed in semilogarithmic coordinates, is a straight line with slope  $a$ :

$$\log_{10} N(E > \varepsilon) \propto -a\varepsilon. \quad (1a)$$

Correlation (1a) is equivalent to the Poisson-type exponential law:

$$N(E > \varepsilon) \propto \exp(-a\varepsilon). \quad (1b)$$

The distributions  $N(E > \varepsilon)$  versus  $\varepsilon$  for a bombarded specimen of  $\alpha$ -quartz (SiO<sub>2</sub><sup>amorphiz</sup>, Fig. 3, b), as well as specimens of  $v$ -SiO<sub>2</sub> before and after implantation (Fig. 3, c),

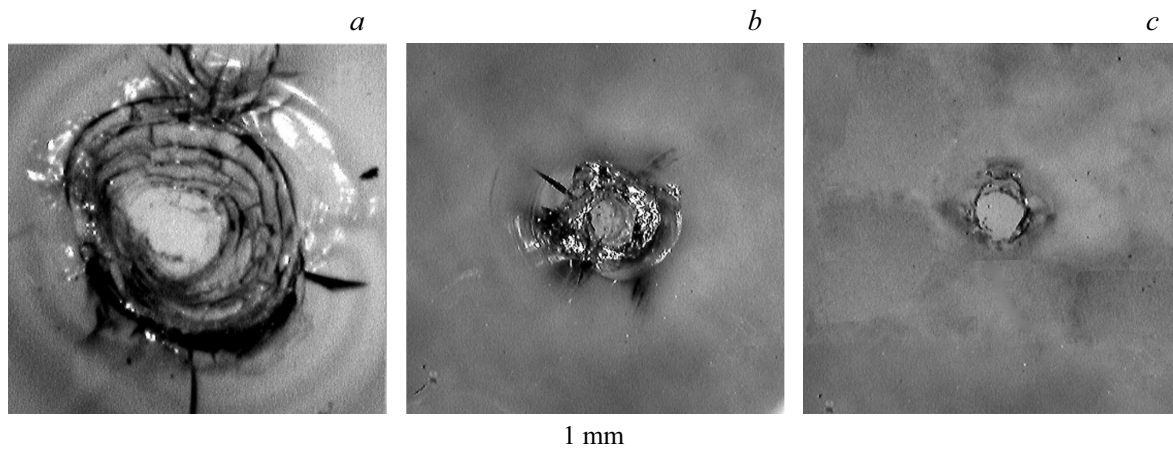


**Figure 2.** Optical photographs of the damage to the specimen surface caused by the striker  $v\text{-SiO}_2$  (a),  $\alpha\text{-SiO}_2$  (b) and  $\text{SiO}_2^{\text{amorphiz}}$  (c).

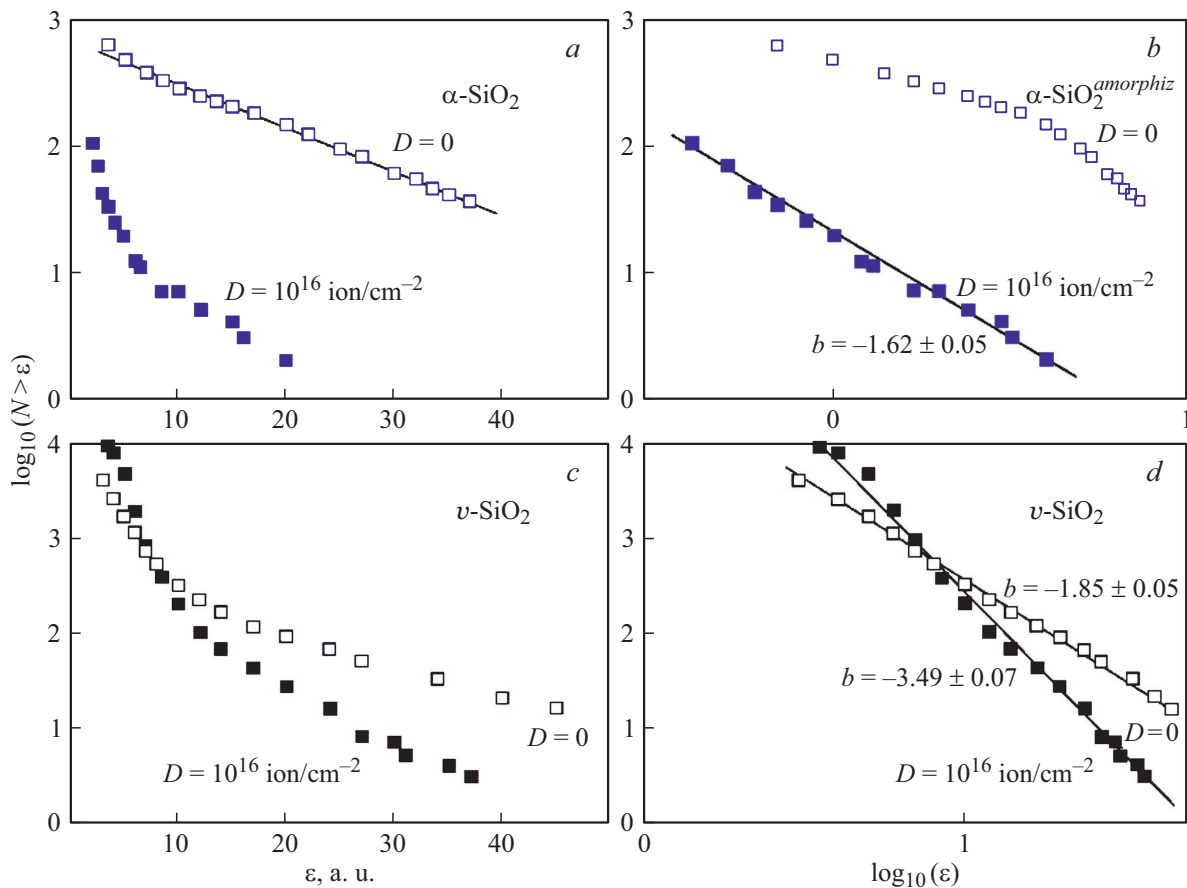


**Figure 3.** Energy distributions in ML pulses with implantation doses ( $D$ ). The figure shows the number of pulses whose energy exceeds the value given at the corresponding abscissa point:  $a, c$  are semilogarithmic coordinates;  $b, d$  are double logarithmic coordinates. The straight line on the panel (a) satisfies the exponential law (correlation (1b)); the straight lines on the panels (b, d) satisfy the power law (correlation (2b)).

plotted in a semilogarithmic scale, are represented by descending curves having no linear areas of the type of correlation (1 a) and cannot be described by any elementary function. However, since they were plotted in log–log-coordinates, these distributions have showed log-linear

dependences:

$$\log_{10}(E > \epsilon) \propto -b \log_{10}(\epsilon), \quad (2a)$$

where  $b$  is slope of straight segments.

By clearing the logarithms from correlation (2a), we obtain a distribution of energies in ML pulses in the form of a power law:

$$N(E > \varepsilon) \propto \varepsilon^{-b}. \quad (2b)$$

## 4. Discussion

The exponential law (1b), obtained for the energy distribution in ML pulses under impact loading of non-bombarded  $\alpha$ -quartz (Fig. 3, *a*), is typical for random events occurring independently of each other. The correlation radius of environment disturbance by the caused defect is smaller than the distance between potentially „weak“ spots — disruptions of the crystalline order (if such are present). The ions in the bombarded  $\text{SiO}_2^{\text{amorphiz}}$  crystal have generated many broken bonds which interacted under the load and new defects formed. Energy yield was according to the power law typical for cooperative phenomena (Fig. 3, *b*).

At the same time, the energy distribution in the ML series under impact loading of non-bombarded vitreous  $v$ - $\text{SiO}_2$  has also (as distinct from the non-implanted crystalline quartz) followed the power law (Fig. 3, *d*). This is due to variations of the relative position of siloxane rings in relation to each other, which create a distribution of deviations of Si—O—Si angles from the equilibrium value. Thus, given the structural heterogeneity of  $v$ - $\text{SiO}_2$ , it has a distribution of „weak“ spots interacting in the force field even in a non-bombarded material.

Parameter  $b$  (slope of straight lines) in the power dependences characterizes the relative contribution of „major“ and „minor“ events to the overall energy distribution. The lower the value of  $b$ , the more major events contribute to the distribution  $N(E > \varepsilon)$  versus  $\varepsilon$ . Based on this criterion, it can be seen that ML emission from the amorphized crystal (Fig. 3, *b*) occurs with a higher energy yield than that from a bombarded amorphous (vitreous)  $v$ - $\text{SiO}_2$  (Fig. 3, *d*) both before and after implantation of the latter. At the same time, the ion implantation-induced increase in density of structural defects in  $v$ - $\text{SiO}_2$  has caused a redistribution of energy in the impact-induced ML pulses in favor of minor events (parameter  $b$  has increased from 1.85 to 3.49 (Fig. 3, *d*)).

## Conclusion

The fractoluminescence method was used to study the degradation of both crystalline and amorphous modifications of silicon dioxide upon fracture. We have compared specimen behavior before and after implantation of  $\text{Ar}^+$  ions, which created multiple  $[\equiv \text{Si}-\text{O}^-]$  groups in the surface layer. It has been shown that the formation of primary defects in crystalline quartz upon impact fracture of non-bombarded specimens was random, i.e. new defects did not influence new bond breaks. Defects in the „amorphized“ specimen of ( $\text{SiO}_2^{\text{amorphiz}}$ ) with a high concentration of bonds, broken by ions, were accumulated according to the cooperative scenario.

Accumulation of breaks of the silicon-oxygen framework in vitreous (molten) quartz, due to its heterogeneity at the level of the medium-range order (non-ordered mesh of siloxane rings), took place with interactions inside the defect ensemble both before and after bombardment.

## Conflict of interest

The authors declare that they have no conflict of interest.

## References

- [1] H. Fischer, G. Götz, H. Karge. *PSS*, **76**, 249 (1983). DOI: org/10.1002/pssa.2210760211
- [2] L. Douillard, J.P. Duraud. *Nucl. Instrum. Meth. B*, **107**, 212 (1996). DOI.org/10.1016/0168-583X(95)01044-0
- [3] S. Gąsiorek, K.P. Lieb, P.K. Sahoo, Keinonen *J. Appl. Phys. B*, **93**, 245 (2008). DOI: 10.1007/s00340-008-3156-6
- [4] P.K. Gupta. *J. Non-Cryst. Solid.*, **195**, 158 (1996). DOI: org/10.1016/0022-3093(95)00502-1
- [5] D. Shamiryanyan, D.V. Likhachev. *Spectroscopic Ellipsometry of Ion-Implantation-Induced Damage*. In: Ion Implantation. Ed. M. Goorsky (InTech, Rijeka, Croatia, 2012), p. 89–104.
- [6] P.C. Basu, P. Labbé, D.J. Naus. 22nd Conf. on Structural Mechanics in Reactor Technology, Division 6. San Francisco, USA, 2013.
- [7] E.I. Rau, A.A. Tatarintsev, E.Yu. Zykova, S.V. Zaitsev. *ZhTF*, **89**, 13 (2019) (in Russian). DOI: 10.21883/JTF.2019.08.47904.264-18
- [8] C.R. Fritzche, W.R. Rothmund. *J. Electrochim. Soc.*, **119**, 1243 (1972).
- [9] I.P. Scherbakov, A.E. Chmel. *FKhS*, **46**, 509 (2020) (in Russian). DOI: 10.31857/S013266512005008X